Mechanical and Rheological Properties of the Maleated Polypropylene–Layered Silicate Nanocomposites with Different Morphology

Chong Min Koo,[1] Mi Jung Kim,[1] Min Ho Choi,[2] Sang Ouk Kim,[3] In Jae Chung[1]

[1]*Department of Chemical and Biomolecular Engineering, Korea Advanced Institute of Science and Technology, 373-1, Kusong-dong, Yusong-gu, Taejon 305-701, South Korea*
[2]*Department of Materials Science and Engineering, Cornell University, Ithaca, New York 14853*
[3]*Department of Chemical Engineering, University of Wisconsin at Madison, 2020 Engineering Hall, 1415 Engineering Drive, Madison, Wisconsin 53706*

Received 25 March 2002; accepted 13 July 2002

ABSTRACT: Three types of maleated polypropylene–layered silicate nanocomposites with different dispersion states of layered silicate (deintercalated, intercalated, and exfoliated states) are prepared from two kinds of polypropylenes with different molecular weights, organically modified layered silicate and pristine montmorillonite to investigate the effect of the final morphology of the nanocomposite on the rheological and mechanical properties. Maleated polypropylene with high molecular weight intercalates slowly and the other with low molecular weight exfoliates fast into the organophilic layered silicates. Rheological properties such as oscillatory storage modulus, nonterminal behavior, and relative viscosity has close relationship with the dispersion state of layered silicates. The exfoliated nanocomposite shows the largest increase and the deintercalated nanocomposite shows almost no change in relative shear and complex viscosities with the clay content. The exfoliated nanocomposite shows the largest drop in complex viscosity due to shear alignment of clay layers in the shear flow. In addition, the final dispersion state of layered silicates intimately relates to the mechanical property. The dynamic storage moduli of nanocomposites show the same behavior as the relative shear and complex viscosities. © 2003 Wiley Periodicals, Inc. J Appl Polym Sci 88: 1526–1535, 2003

Key words: nanocomposites; morphology; rheology

INTRODUCTION

Polymer-layered silicate nanocomposites (PLSNs) have attracted a great deal of attention due to their academic and industrial importance. They have shown dramatic improvements in mechanical, thermal, and barrier properties with a small amount of layered silicates.[1–22] Moreover, they give a model system not only on the studies of the polymer chain dynamics in the confined geometry,[23–33] but also on the thermodynamic phase behavior of polymer–nanoparticle mixture.[34–39]

A PLSN may have one of three morphologies. Deintercalated structure has the aggregation of layered silicate with which polymer is immiscible. Intercalated structure has well-ordered multilayers in which the extended polymer chains are inserted. Exfoliated structure results in the separation of silicate layers keeping the gap between layers wide enough for no interaction between the adjacent layers.

The tightly stacked clay sheets with smaller gallery height than the radius of gyration of a typical polymer act as a crucial geometric limit that inhibits the polymer chains from penetrating into and becoming intermixed with the layers of clay.[31–36] A number of studies reported that the favorable enthalpic interaction balance between layered silicate and matrix polymer acts as a decisive role in overcoming the geometrical limit. A handful of the studies have investigated on entropic effect such as the difference of molecular weight effect of matrix resin in the fabrication of the nanocomposites and reported that the entropic effect to the final morphology is negligible.[23–25] On the other hand, it has been reported that the increase in the polymer chain length can lead to high immiscibility between clay and polymer.[31–36] This implies that final morphology of nanocomposites can be affected by the molecular weight of matrix polymer.

In addition, the final morphology can influence the mechanical and rheological properties of PLSNs. The studies on PLSNs have shown a significant change in the viscoelastic property depending on their microstructure and the interfacial characteristics between polymer and layered silicate.[22–33] Hoffmann et al.[30] and Lim and Park[32] reported that the linear viscoelastic property in nanocomposites was highly affected by the final dispersion state of clay in the polymer matrix.

Correspondence to: In Jae Chung (chung@kaist.ac.kr).
Contract grant sponsor: Brain Korea 21 program.
Contract grant sponsor: the Center for Advanced Functional Polymers.

TABLE I
Characterization of Two Types of Maleated Polypropylene

	HMPP	LMPP
T_m[a] (°C)	159.1	156.9
M_w[b]	185,000	59,000
Poly Dispersity Index (PDI) (M_w/M_n)[b]	5.6	2.3
Graft level (%)		
$A_{C=O}/A_{1170}$	1.9	1.8
^{1}H NMR[c]	2.4	2.0
Elemental analysis	1.9	1.9

[a] Obtained from second heating scan with heating rate of 10°C/min.
[b] Measured by Gel Permeation Chromatography (GPC).
[c] Calculated by ^{1}H NMR.

In particular, the nanocomposites with the polymer chains end-tethered on the surface of silicate showed significant change in the viscoelastic properties.[26,27] Owing to the limited number of model systems, however, the morphological effect throughout the mechanical and rheological properties is less well investigated.

On this account, maleated polypropylene–layered silicate nanocomposite is used as a model system for the study of the effect of morphology of the nanocomposites on the rheological and mechanical properties. The molecular weight difference of maleated polypropylene matrix influenced not only intercalation kinetics but also final morphology of the nanocomposite. Here the mechanical and rheological properties of nanocomposites with different morphologies are investigated.

EXPERIMENTAL

Materials

Two types of layered silicates were used: pristine montmorillonite (MMT) and organophilic montmorillonite (C18M) modified with stearylamine (Nanocor). The cationic exchange capacity (CEC) of MMT was 108 meq/100 g. Two types of maleated polypropylene (HMPP with M_w of 185,000 and LMPP with M_w of 59,000) used in this work are listed in Table I. Detailed properties of maleated polypropylenes were reported in a previous study.[12] They have the same grafting

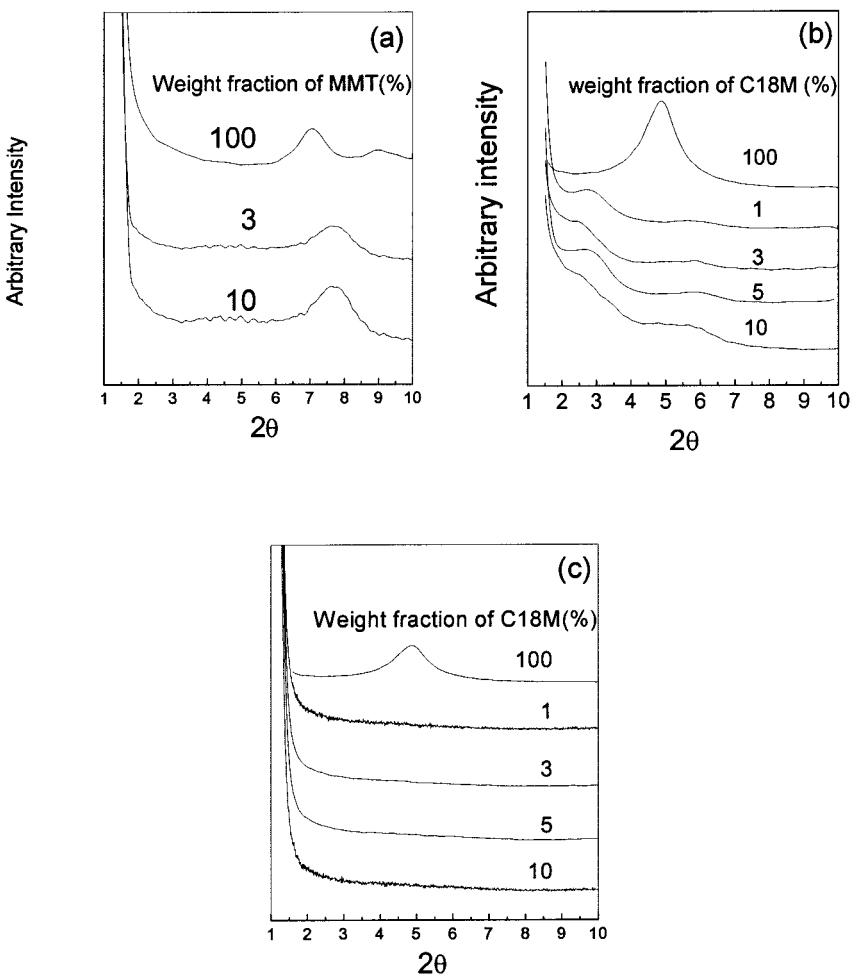

Figure 1 XRD patterns of (a) HMPP–MMT, (b) HMPP–C18M, and (c) LMPP–C18M with different amounts of clay.

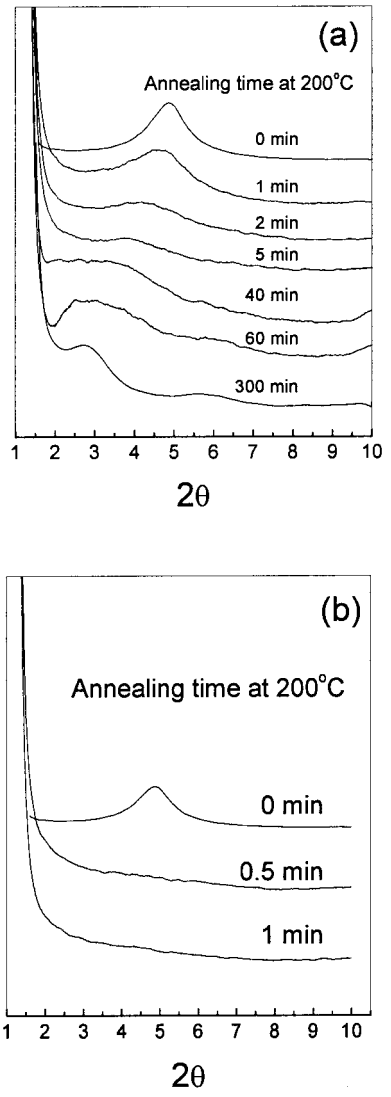

Figure 2 XRD patterns of (a) HMPP–C18M3 and (b) LMPP–C18M3 as a function of annealing time at 200°C.

content of maleic anhydride (MA) and different molecular weights. The three types of maleated polypropylene–layered silicate nanocomposites (HMPP–MMT, HMPP–C18M, and LMPP–C18M) have been prepared by typical melt intercalation method for 20 min at 200°C. The notation HMPP–C18M10 indicates HMPP–C18M nanocomposite with C18M of 10 wt %.

Measurement

The intercalation kinetics and intercalation capability of the nanocomposites were evaluated by X-ray diffractometer (Rigaku X-ray generator, CuKα radiation, $\lambda = 0.15406$ nm). The final dispersion state of layered silicates was measured by transmission electron microscopy (TEM; Philips CM-20 transmission electron microscope). All rheological measurements were performed on Rheometric Scientific, ARES, a strain-controlled rheometer, with cone and plate geometry in oscillatory and steady-shear modes. The plates had a diameter of 50 mm and a cone angle of 0.04 rad. All measurements were carried out under nitrogen at 200°C. Linear viscoelastic measurements before and after sufficient steady shear were performed in order to investigate the shear-aligning behavior of the nanocomposites. The steady shear rate was applied at $\dot{\gamma} = 1\ s^{-1}$ for 20 min. The shear-aligned microstructure in the nanocomposite was measured by using 2D SAXS photographs in Pohang Light Sources (PLS), Korea. Dynamic viscoelastic properties were measured using a DMA (Universal V2.5H TA Instruments). The dynamic storage moduli of the nanocomposites were determined at 10 Hz in the temperature range between −100 and 100°C.

RESULTS AND DISCUSSION

Final morphology and intercalation kinetics in nanocomposites

Figure 1 shows the XRD patterns of HMPP–MMT, HMPP–C18M, and LMPP–C18M nanocomposites with the amounts of clay. The peak in XRD patterns corresponds to the (001) reflection peak of layered

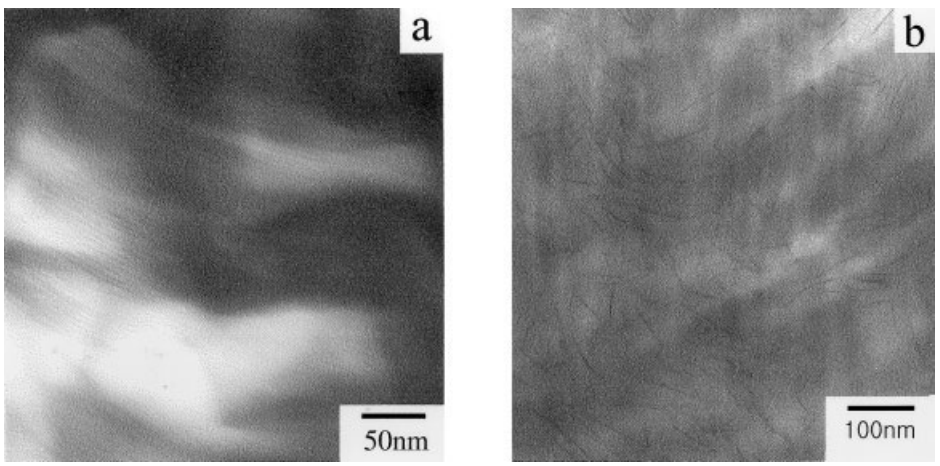

Figure 3 Transmission electron micrographs of (a) HMPP–C18M10 and (b) LMPP–C18M10.

TABLE II
Characterization of MMT, C18M, and Maleated Polypropylene–Clay Nanocomposites

Wt % clay	Sample	Morphology (2θ = d-spacing)	Sample	Morphology (2θ = d-spacing)	Sample	Morphology
100	MMT	(7.03° = 1.26 nm)	C18M	(4.87°=1.8nm)	C18M	(4.87° = 1.8 nm)
1		—	HMPP–C18M1	Intercalated (2.74° = 3.2 nm)	LMPP–C18M1	Exfoliated
3	HMPP–MMT3	Deintercalated (7.70° = 1.15 nm)	HMPP–C18M3	Intercalated (2.5° = 3.5 nm)	LMPP–C18M3	Exfoliated
5		—	HMPP–C18M5	Intercalated (2.66° = 3.3 nm)	LMPP–C18M5	Exfoliated
10	HMPP–MMT10	Deintercalated (7.67° = 1.15 nm)	HMPP–C18M10	Intercalated (2.45° = 3.6 nm)	LMPP–C18M10	Exfoliated

HMPP and LMPP = maleated polypropylene with high molecular weight (M_w = 185,000) and low molecular weight (M_w = 59,000), respectively.

silicates. In Figure 1(a), the d-spacing of MMT calculated by using Bragg's law is about 1.26 nm. The d-spacings in HMPP–MMT nanocomposites are nearly the same as that of MMT. It indicates that HMPP–MMT has the deintercalated morphology, which may result from the immiscibility between HMPP and MMT. In Figure 1(b), the layer spacing of C18M is about 1.8 nm, while HMPP–C18M nanocomposites have the layer spacing between 3.2 and 3.6 nm. XRD pattern of HMPP–C18M represents successful intercalation of HMPP into C18M. In Figure 1(c), LMPP–C18M nanocomposites do not have the characteristic plane peak, which indicates the exfoliation of the layered silicates. The XRD patterns do not change with clay content.

Figure 2 shows the XRD patterns of HMPP–C18M and LMPP–C18M nanocomposites with 3 wt % C18M at various annealing time at 200°C. Mixture of HMPP

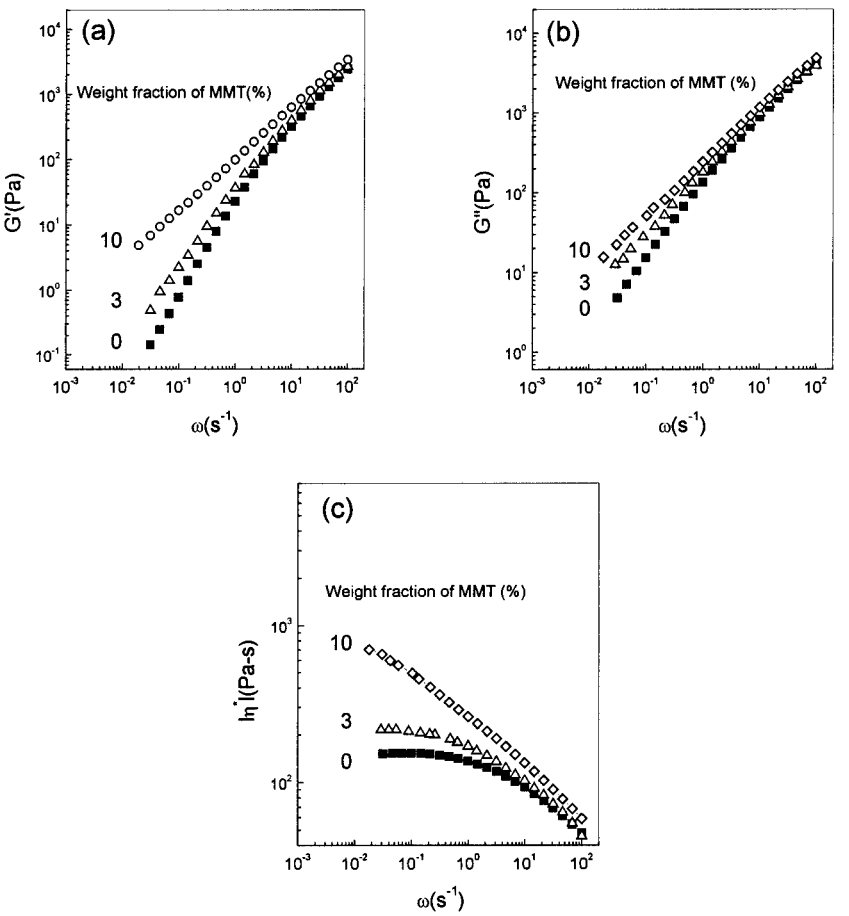

Figure 4 Graphs of (a) storage modulus, (b) loss modulus, and (c) complex viscosity for HMPP–MMT nanocomposites at 200°C.

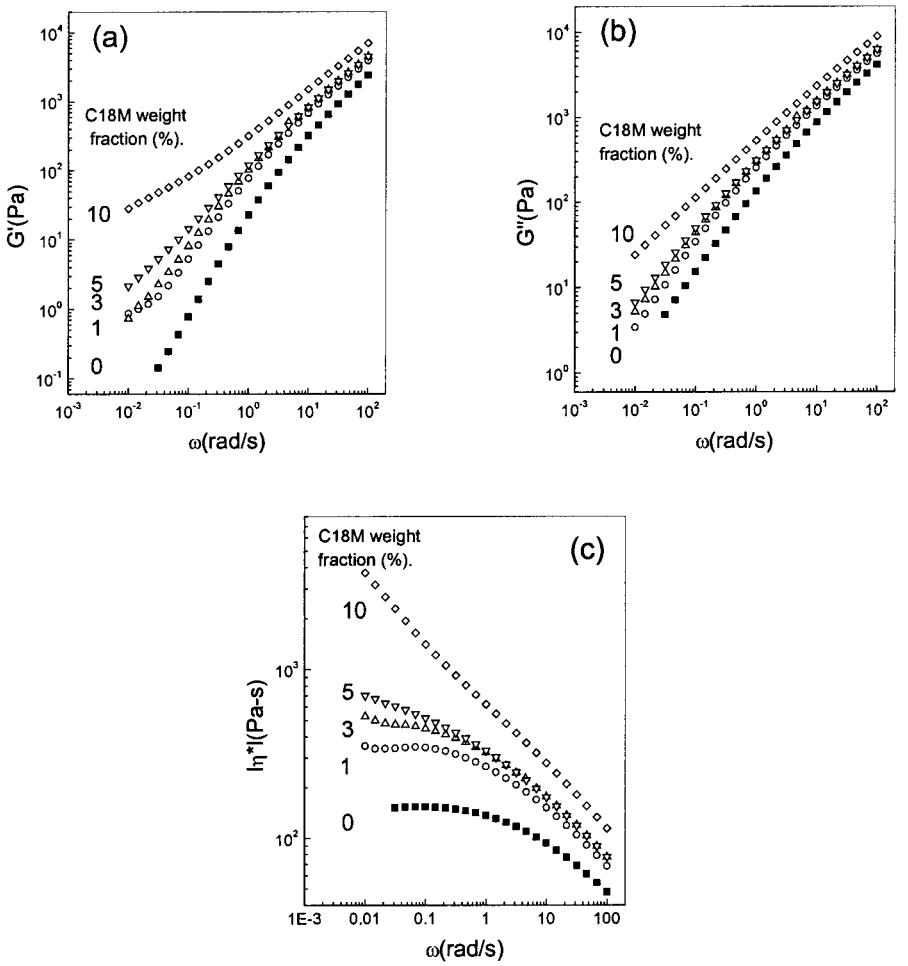

Figure 5 Graphs of (a) storage modulus, (b) loss modulus, and (c) complex viscosity for HMPP–C18M nanocomposites at 200°C.

and C18M is mechanically premixed and annealed in molder for XRD experiment. When the mixture of HMPP and C18M is annealed at 200°C, it takes about 1 h to complete the intercalation. The (001) reflection peak is gradually shifted from 4.9° to 2.6° until 1 h. The plane peak no longer shifts with further annealing. On the contrary, Intercalation kinetic behavior of LMPP–C18M nanocomposites is quite different from that of HMPP–C18M nanocomposites. In the case of LMPP–C18M nanocomposites, even annealing for 30 s makes the (001) reflection peak disappear. It can be concluded that HMPP with high molecular weight intercalates slowly and LMPP with low molecular weight exfoliates fast into the C18M. The results indicate the slow penetration of polymer chains with a high molecular weight into silicate layers and the low miscibility between polymer chains with high molecular weight.[34–39]

Figure 3 shows transmission electron micrographs of HMPP–C18M10 and LMPP–C18M10 nanocomposites. Dark lines represent the silicate layers. In Figure 3(a), HMPP–C18M shows the stacked silicate layers. The average size of the stacked tactoid ranges from 40 layers to over 100 layers and the layer spacing is about 3.5 nm. It indicates that HMPP successfully intercalates into C18M. On the other hand, in Figure 3(b), one can observe that layers of C18M are clearly exfoliated by the LMPP. Typical layers are 100–300 nm in length and 1 nm in thickness. These results agree well with those of XRD. The three types of the nanocomposites are characterized in Table II.

Final morphology and rheology

Storage moduli, loss moduli, and complex viscosities (G', G'', and η^*, respectively) of HMPP–MMT, HMPP–C18M, and LMPP–C18M nanocomposites measured at 200°C are given in Figures 4–6, respectively. The curves of G' and G'' for each nanocomposite series show monotonic increase with the concentration of clay at all frequency and show the higher increase of storage modulus at a high frequency than at a low frequency. The change of the viscoelastic properties shows the intimate relationship with their morphologies. To consider the relationship between the final morphology and the rheological behavior of the nanocomposites, relative complex viscosity (η^*_{re}) and the

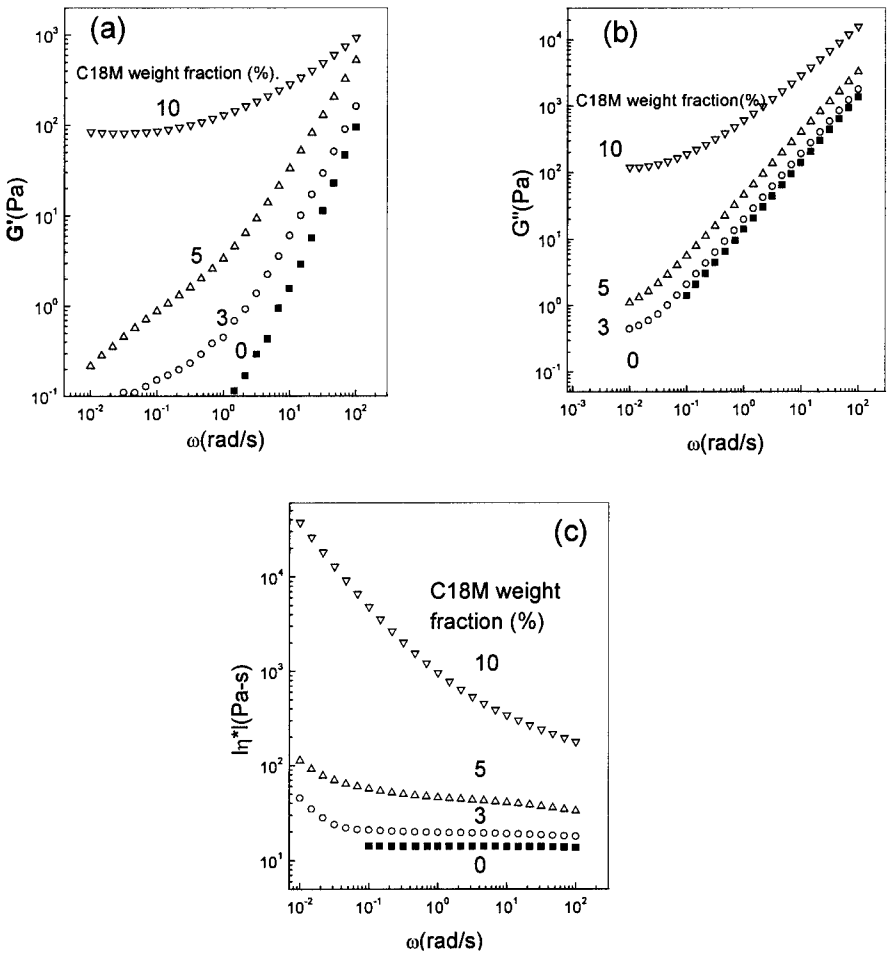

Figure 6 Graphs of (a) storage modulus, (b) loss modulus, and (c) complex viscosity for LMPP–C18M nanocomposites at 200°C.

relative steady shear viscosity (η_{re}) are investigated in Figures 7 and 8, respectively. η^*_{re} at $\omega = 100\ s^{-1}$ is obtained from Figures 4–6. η_{re} is obtained at shear rate of $\dot{\gamma} = 1\ s^{-1}$, which is Newtonian plateau region for both HMPP and LMPP. Both η^*_{re} and η_{re} are highly dependent not only on the concentration of clay but also on the final morphology. In particular, η^*_{re} and η_{re} of the exfoliated LMPP–C18M show the steepest increase with the concentration of clay. The intercalated HMPP–C18M shows steeper increase than the deintercalated HMPP–MMT.

The terminal slopes of all samples are listed in Table III. All nanocomposites exhibit nonterminal behavior in the low-frequency region. The change of terminal slopes also depends on both the concentration of clay and the morphology of nanocomposite. A monodisperse polymer has two and one slope of G' and G'', respectively. LMPP has 1.61 and 1 and HMPP has 1.51 and 0.98, which might be attributed to their wide molecular weight distribution.[40] Terminal slopes decrease with the increase in clay concentration. The exfoliated LMPP–C18M has the faster decreasing rate of slopes than HMPP–C18M. On the other hand, the deintercalated HMPP–MMT is the least sensitive to terminal slopes with the concentration of clay.

The intimate relationship between final morphology and the rheological properties results from the microstructural difference as well as the interfacial characteristics between silicate layers and polymer.[26,27,32,33] In particular, the better dispersibility of the layered silicate in the PLSN is responsible for the higher increase in the effective surface area of the layered silicates as well as the probability of the particle–particle interaction. As shown in Figure 3, individual silicate layers with high aspect ratio are homogeneously dispersed in the LMPP–C18M. But they are still stacked in HMPP–C18M. Hence, the exfoliated LMPP–C18M with best dispersibility of layered silicates shows the largest increase in relative shear viscosity and complex viscosity. In particular, LMPP–C18M with C18M of 10 wt % almost reaches the zero slope of dynamic moduli in a low frequency region, as shown in Figure 6. It indicates that the exfoliated LMPP–C18M forms the percolated network structures of the layered silicates at the lowest silicate loading due to the largest effective anisotropy.[29,30,32,33]

Rheology of shear-induced alignment

From the processing and application point of view, the shear-induced alignment of the filler with anisotropic

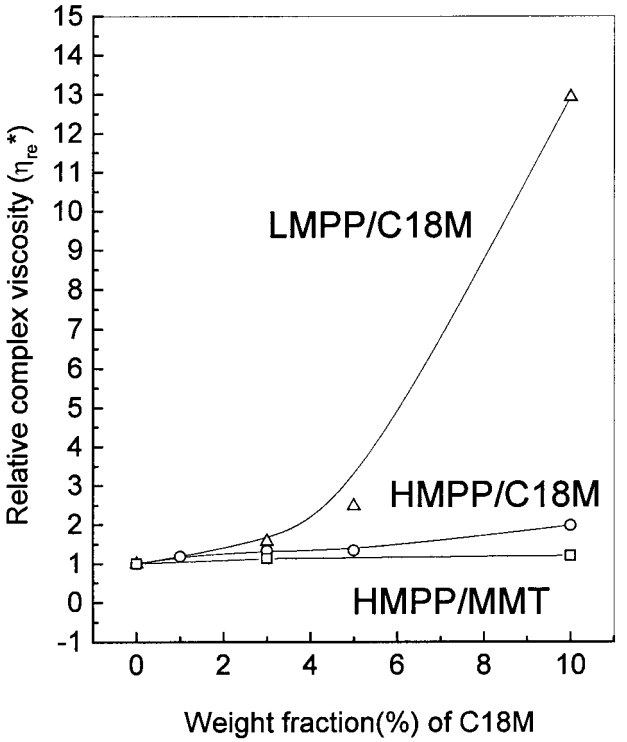

Figure 7 Relative complex viscosity of HMPP–MMT, HMPP–C18M, and LMPP–C18M nanocomposites at the frequency of 100 s^{-1}.

shape in the composite is very significant. The layered silicates with anisotropic shape in nanocomposite could be aligned by the application of large-amplitude

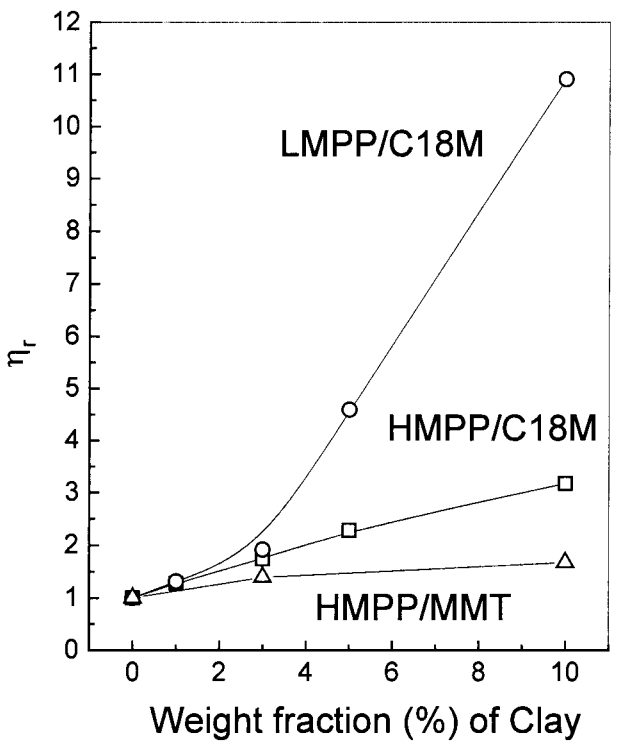

Figure 8 Relative steady shear viscosity of HMPP–MMT, HMPP–C18M, and LMPP–C18M nanocomposites at the shear rate of 1 s^{-1}.

TABLE III
Terminal Slopes of G' and G'' vs. ω for the Nanocomposites

Clay content (wt %)	HMPP–MMT		HMPP–C18M		LMPP–C18M	
	G′	G″	G′	G″	G′	G″
0	1.51	0.98	1.51	0.98	1.61	1.00
1			0.96	0.97	1.10	0.97
3	1.24	0.96	1.08	0.91	0.61	0.88
5			0.85	0.84	0.58	0.76
10	0.78	0.70	0.48	0.67	0.00	0.17

oscillatory shear or steady shear.[26,27,29,31] Figure 9 shows the 2D SAXS patterns of LMPP–C18M with 10 wt % C18M before and after steady shear. Flow direction corresponds to the meridian in images. We can see a reflection on the equator near the beam stopper. It is a typical 2D SAXS image of the exfoliated nanocomposite.[41,42] The nanocomposite without shear shows the isotropic intensity distribution, while the nanocomposite with shear shows strongly anisotropic intensity distribution on the meridian. It indicates that

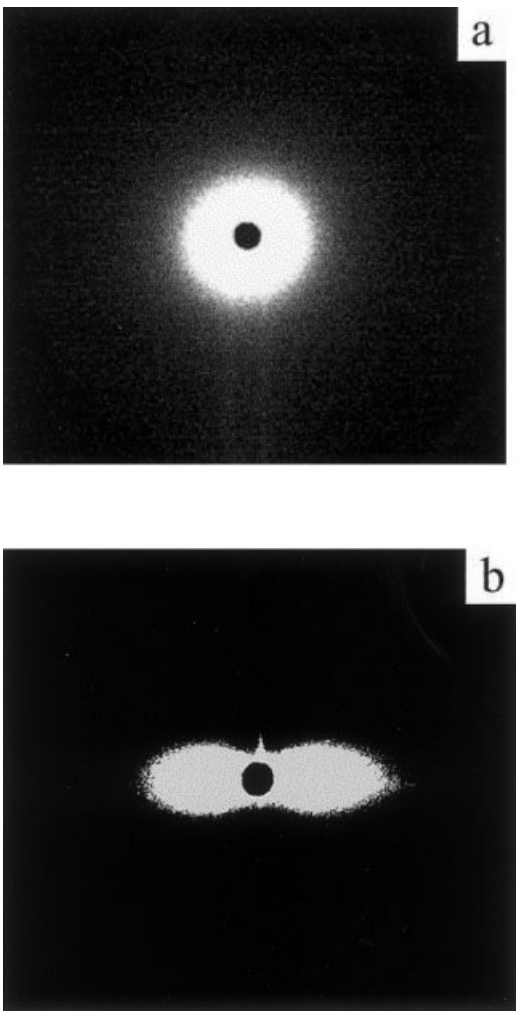

Figure 9 Two-dimensional SAXS patterns of LMPP–C18M with 10 wt % C18M (a) before and (b) after steady shear.

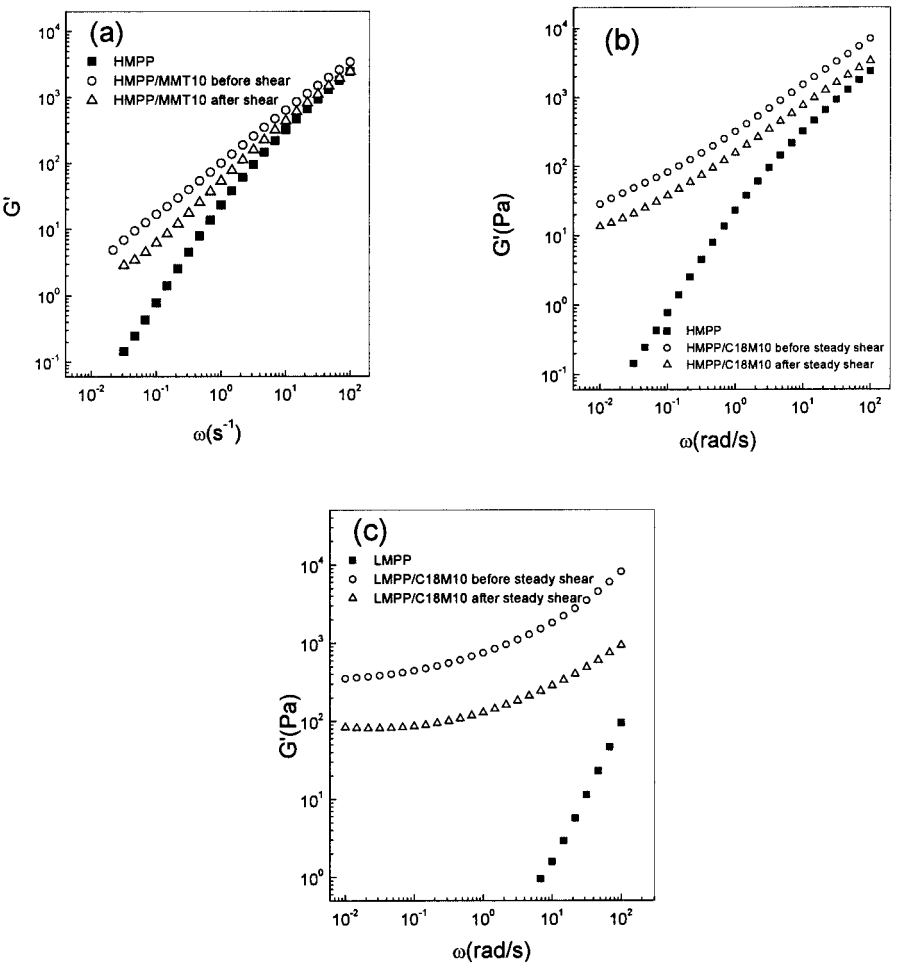

Figure 10 Storage modulus (G') for (a) HMPP–MMT10, (b) HMPP–C18M10, and (c) LMPP–C18M10 nanocomposites before and after sufficient steady shear.

the silicate layers are randomly distributed before shear is applied, but they are highly oriented in the flow direction under the shear in the nanocomposite. Such microstructural change may induce a significant change of rheological property.

Figure 10 shows G' of HMPP–MMT10, HMPP–C18M10, and LMPP–C18M10 nanocomposites before and after sufficient steady shear. Steady shear rate was applied at $\dot{\gamma} = 1\ s^{-1}$ in the Newtonian plateau region for HMPP and LMPP for 20 min. G' decreases with the shearing time and reaches a constant value. The disorientation of the aligned nanocomposites did not appear in the oscillatory experiment. The aligned nanocomposite has the lower G' than the initially unaligned one at all frequencies. To elucidate the relationship between final morphology and shear-induced alignment, complex viscosity drops are summarized in Table IV. LMPP–C18M has the largest drop in complex viscosity and HMPP–C18M has the next drop and HMPP–MMT has the smallest drop. The complex viscosity drop of a nanocomposite is from the difference of complex viscosity between the random state and the aligned state. Shear rate 1 s^{-1} is Newtonian plateau region for both HMPP and LMPP. Therefore, it must be due to the orientation of the layered silicates. The nanocomposite containing the filler with higher effective aspect ratio may produce the higher complex viscosity drop.[7] The nanocomposite with sphere particles may not show shear alignment.

Final morphology and mechanical properties

The dynamic storage moduli (E') of nanocomposites are given in Figure 11. HMPP–C18M and LMPP–C18M nanocomposites show abrupt improvement in

TABLE IV
Complex Viscosity Drops of HMPP–MMT10, HMPP–C18M10, and LMPP–C18M10 After Sufficient Steady Shear

	Complex viscosity drop, $\Delta(\log(\eta^*))$		
	1 s^{-1}	10 s^{-1}	100 s^{-1}
HMPP–MMT10	0.15	0.09	0.11
HMPP–C18M10	0.28	0.29	0.31
LMPP–C18M10	0.79	0.89	1.02

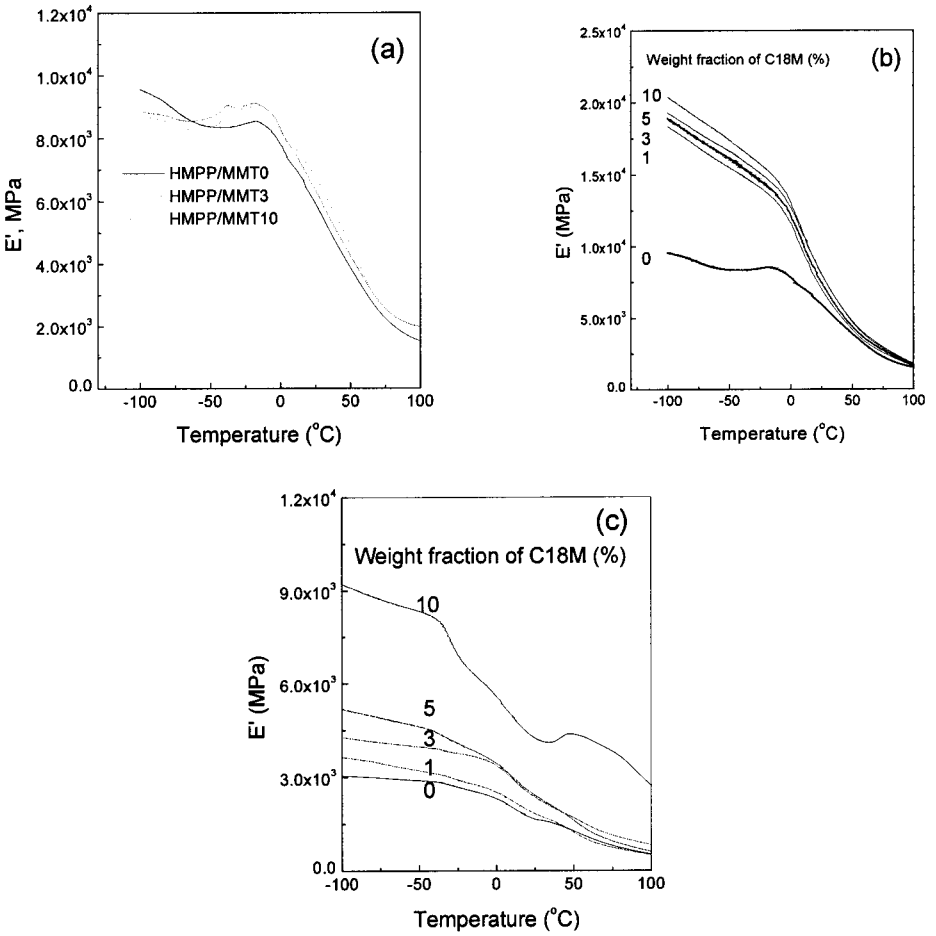

Figure 11 Dynamic storage moduli (E') of (a) HMPP–MMT, (b) HMPP–C18M, and (c) LMPP–C18M as a function of temperature.

the dynamic storage modulus as the concentration of clay increases when compared to HMPP and LMPP. However, HMPP–MMT shows slight increase in E' relative to HMPP. To consider relationship between final morphology and E' of nanocomposites, relative dynamic storage moduli of nanocomposites to the matrix polymer at 30°C are plotted in Figure 12. The exfoliated nanocomposite shows the largest increase in E'/E'_o, as expected from the result of relative viscosity.[7]

CONCLUSIONS

HMPP with high molecular weight intercalated slowly and LMPP with low molecular weight exfoliated rapidly into the C18M. LMPP–C18M nanocomposites exhibit exfoliated structures, HMPP–C18M nanocomposites exhibit intercalated structures, and HMPP–MMT composites exhibit deintercalated structures. Exfoliated nanocomposite shows the largest increase, intercalated a moderate increase, and deintercalated the smallest increase in relative shear and complex viscosities with the clay content. In addition, the complex viscosity drop is the largest for the exfoliated nanocomposite and the smallest for the deintercalated

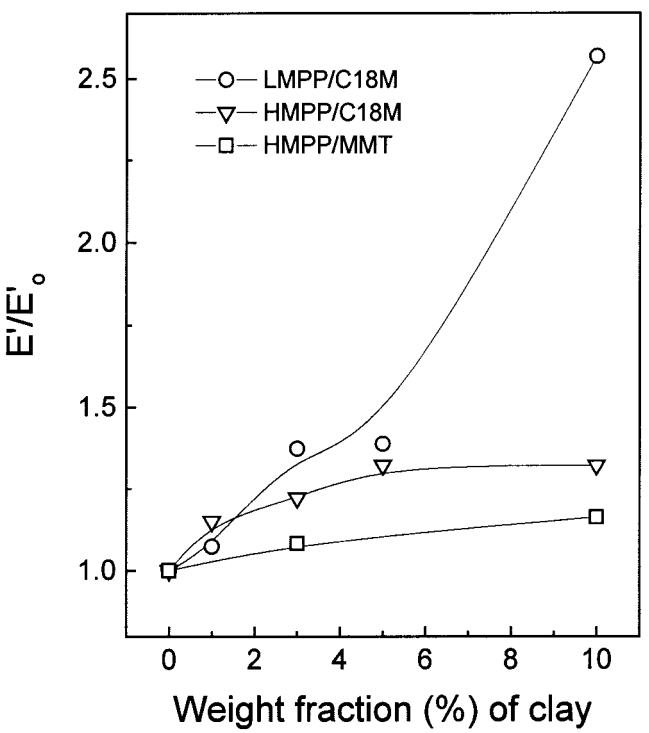

Figure 12 Relative dynamic storage moduli (E'/E'_o–matrix polymer) of three types of nanocomposite series to that of matrix polymer.

composite during the shear flow. The dynamic storage modulus also shows the same behavior as the relative shear and complex viscosities. The rheological and mechanical properties depend largely on the final morphology of nanocomposite and the clay content.

This work was supported in part by the Brain Korea 21 program and in part by the Center for Advanced Functional Polymers. The authors thank Chang-Hyeon Kim and the Honam Chemical Corporation for providing maleated polypropylene resin. This experiment at PLS (Pohang Light Sources) was supported in part by MOST and POSCO.

References

1. Kojima, Y.; Usuki, A.; Kawasumi, M.; Okada, A.; Fukushima, Y.; Kurauchi, T.; Kamigaito, O. J Mater Res 1993, 8, 1185.
2. Kojima, Y.; Usuki, A.; Kawasumi, M.; Okada, A.; Kurauchi, T.; Kamigaito, O. J Appl Polym Sci 1993, 8, 1185.
3. Gilman, J. W. Appl Clay Sci 1999, 15, 31.
4. Giannelis, E. P. Adv Mater 1996, 8, 29.
5. Vaia, R. A.; Vasudevan, S.; Krawiec, W.; Scanlon, S. G.; Giannelis, E. P. Adv Mater 1995, 7, 154.
6. Choi, M. H.; Chung, I. J.; Lee, J. D. Chem Mater 2000, 11, 2977.
7. Wang, K. H.; Xu, M.; Choi, Y. S.; Chung, I. J. Polym Bull 2001, 46, 499.
8. Wang, K. H.; Choi, M. H.; Koo, C. M.; Chung, I. J. Polymer 2001, 42, 9819.
9. Choi, Y. S.; Choi, M. H.; Wang, K. H.; Kim, S. O.; Kim, Y. K.; Chung, I. J. Macromolecules 2001, 34, 8978.
10. Byun, H. Y.; Choi, M. H.; Chung, I. J. Chem Mater 2001, 13, 4221.
11. Koo, C. M.; Ham, H. T.; Kim, S. O.; Wang, K. H.; Chung, I. J.; Kim, D. C.; Zin, W. C. Macromolecules 2002, 35, 5116.
12. Koo, C. M.; Kim, M. J.; Choi, M. H.; Kim, S. O.; Chung, I. J. Hwahak Konghak 2001, 39, 635.
13. Galgali, G.; Ramesh, C.; Lele, A. Macromolecules 2001, 34, 852.
14. Hasegawa, N.; Okamoto, H.; Kato, M.; Usuki, A. J Appl Polym Sci 2000, 78, 1918.
15. Kawasumi, M.; Hasegawa, N.; Kato, M.; Usuki, A.; Okada, A. Macromolecules 1997, 30, 6333.
16. Hasegawa, N.; Kawasumi, M.; Kato, M.; Usuki, A.; Okada, A. J Appl Polym Sci 1998, 67, 87.
17. Kato, M.; Usuki, A.; Okada, A. J Appl Polym Sci 1997, 66, 1781.
18. Usuki, A.; Kato, M.; Okada, A.; Kuraushi, T. J Appl Polym Sci 1997, 63, 137.
19. Kurokawa, Y.; Yasuda, H.; Oyo, A. J Mater Sci Lett 1996, 15, 1481.
20. Krokawa, Y.; Yasuda, H.; Kashiwagi, M.; Oyo, A. J Mater Sci Lett 1997, 16, 1670.
21. Furuichi, N.; Kurokawa, Y.; Fujita, K.; Oyo, A.; Yasuda, H.; Kiso, M. J Mater Sci 1996, 31, 4307.
22. Vaia, R. A.; Sauer, B. B.; Tse, O. K.; Giannelis, E. P. J Polym Sci 1997, 35, 59.
23. Hackett, E.; Manias, E.; Giannelis, E. P. Chem Mater 2000, 12, 2161.
24. Bujdak, J.; Hackett, E.; Giannelis, E. P. Chem Mater 2000, 12, 2168.
25. Vaia, R. A.; Jandt, K. D.; Kramer, E. J.; Giannelis, E. P. Macromolecules 1995, 28, 8080.
26. Krishnamoorti, R.; Vaia, R. A.; Giannelis, E. P. Chem Mater 1996, 8, 1728.
27. Vaia, R. A.; Giannelis, E. P. Macromolecules 1997, 30, 8000.
28. Krishnamoorti, R.; Vaia, R. A.; Giannelis, E. P. Macromolecules 1997, 30, 4097.
29. Ren, J.; Silva, A. S.; Krishnamoorti, R. Macromolecules 2000, 39, 3739.
30. Hoffmann, B.; Dietrich, C.; Thomann, R.; Friedrich, C.; Mulhaupt, R.; Macro Rapid Commun 2000, 21, 57.
31. Lim, Y. T.; Park, O. O.; Macro Rapid Commun 2000, 21, 231.
32. Lim, Y. T.; Park, O. O. Rheol Acta 2001, 40, 220.
33. Hambir, S.; Bulakh, N.; Kodgire, P.; Kalgaonkar, R.; Jog, J. P. J Polym Sci Polym Phys 2001, 9, 446.
34. Lyatskaya, Y.; Balazs, A. C. Macromolecules 1998, 31, 6676.
35. Balazs, A. C.; Singh, C.; Zhulina, E.; Lyatskaya, Y. Acc Chem Res 1999, 32, 651.
36. Ginzburg, V. V.; Singh, C.; Balazs, A. C. Macromolecules 2000, 33, 1089.
37. Ginzburg, V. V.; Balazs, A. C. Adv Mater 2000, 12, 1805.
38. Balazs, A. C.; Singh, C.; Zhulina, E. Macromolecules 1998, 31, 8370.
39. Ginzburg, V. V.; Balazs, A. C. Macromolecules 1999, 32, 5681.
40. Shenoy, A. V. Rheology of filled polymer systems; Kluwer Academic Publishers: New York, 1999.
41. Ogata, N.; Kawakage, S.; Ogihara, T. J Appl Polym Sci 1997, 66, 573.
42. Jimenez, G.; Ogata, N.; Kawai, H.; Ogihara, T. J Appl Polym Sci 1997, 64, 2211.